

Parametric Rietveld refinement of coexisting disordered clay minerals

K. UFER^{1,*} AND R. KLEEBERG²

¹ BGR, Bundesanstalt für Geowissenschaften und Rohstoffe, Stilleweg 2, D-30655 Hannover, Germany

² TU Bergakademie Freiberg, Institute of Mineralogy, 09596 Freiberg, Germany

(Received 15 November 2014; accepted 15 April 2015; Associate Editor: H. Stanjek)

ABSTRACT: X-ray diffraction is one of the most effective tools for the characterization of the stacking defects which occur frequently in clay minerals. Modelling of the diffraction patterns of oriented mounts is often used for obtaining structural information about the nature of stacking order. Manual matching of calculated and observed patterns is time consuming and the results are user dependent and especially troublesome if a consistent model of the same mineral measured under different conditions needs to be obtained. It was shown recently that the Rietveld method could be applied successfully for the evaluation of the X-ray patterns of oriented mounts. Nevertheless, this automatic refinement procedure can also lead to inconsistent results if independent refinements are performed that describe the same sample measured under different conditions. One way to solve this problem is the application of parametric Rietveld refinement. For this approach a set of different measurements of the same sample was collected and fitted in one combined refinement by the connection of the structural models *via* external parameters. These conditions may involve different pre-treatments (e.g. different intercalations), different temperatures or relative humidities and/or different experimental setup (powder or oriented samples). All patterns were fitted in one overall refinement process by the BGMN software.

This approach was demonstrated on a mixture of two disordered reference materials and on a set of geological samples. Two different states for each sample were refined independently and parametrically and it was shown that this approach leads to consistent results, saves computation time and may even resolve small structural differences.

KEYWORDS: Rietveld method, stacking disorder, parametric refinement, BGMN.

Typically, clay minerals show various types of disorder, e.g. planar defects like translational and rotational stacking faults, defects in the order of cation site occupation and possibly interstratification (Drits & Tchoubar, 1990). Although such structural imperfections may complicate structure and phase analysis, knowledge of the type and degree of disorder may provide useful information for geological interpretations, e.g. the reconstruction of the history of sedimentation and diagenesis in sedimentary units.

A traditional method for characterization of clay minerals includes the analysis of one-dimensional diffraction patterns obtained from oriented samples. Ideally, such samples show only the basal 001 series of the typically platy clay minerals. Of course the analysis of polytypes and translational or rotational disorder is impossible from one-dimensional diffraction patterns and a full structural analysis is only possible from non-oriented samples. However, the patterns contain mainly information about the types and order of layers in the direction of stacking, perpendicular to the layer surface. The intensity profile varies as a function of the z-coordinates and may also contain valuable information such as the occupation/substitution of structural sites like the octahedral or interlayer

* Email: Kristian.ufer@bgr.de

DOI: 10.1180/claymin.2015.050.3.03

positions. The enhancement of intensity by orientation, the simple preparation of clay films and the relatively easy and quick calculation of the one-dimensional patterns are advantageous for routine application in clay-mineral analysis.

Manual fitting of one-dimensional diffraction patterns became popular with the publication of computing routines for explicit calculation and these were followed by specialized software programs (Reynolds, 1983, 1985). The analysis procedure consists of the manual variation of the structure model and comparison of the calculated pattern with the measured one. However, this method requires profound understanding of the physical and crystallographic basics, can be time consuming and may give non-unique and user-dependent solutions for complicated systems. A valid method for cross-checking the plausibility of the solutions obtained by manual fitting involves comparing the fit of the same structural model to two or more specimens of the same sample material in different chemical environments, e.g. by changing the interlayer cation or by ethylene glycol saturation (Sakharov *et al.*, 1999). This approach enhances the validity of the interpretation but takes a lot of time and depends on the user's skill.

In recent years the Rietveld method was extended by the parametric refinement approach (Stinton & Evans, 2007; Rajiv *et al.*, 2011). This consists of the simultaneous refinement of several data sets instead of independent refinements. This approach is necessary for comprehensive structural models that explain different sample states. The simplest case of the 'parametric' approach consists of the refinement of global structural variables using a number of different measurements of the same sample. Thus, just adding more information to the refinement of the same set of parameters can help to reach the true global minimum.

Structural parameters, such as lattice parameters or occupancies, can be functions of external parameters such as temperature, pressure or chemical pre-treatment; a typical example from material science is the changes in unit-cell parameters as a function of temperature (Stinton & Evans, 2007). In contrast, the so-called 'non-crystallographic' parameters may be refined from such multiple data sets, e.g. thermal expansion coefficients. In this case, the functional relationship between the individually (for each data set) refined parameters, e.g. lattice parameters and the material property, e.g. thermal expansion, can be used as a constraint and the parameter under question can be derived. In general, the data sets may consist of measurements with different devices, or different

preparation techniques, sample pre-treatments etc. The advantages of this approach are the addition of information by including more measured data, the reduction in the number of independent parameters to avoid correlations running into false refinement minima and, finally, the prevention of inconsistent results.

The aim of the present study is to demonstrate the applicability of the parametric refinement approach in clay mineralogy.

MATERIALS AND METHODS

The performance of parametric refinements is tested by a comparison of independent sequential refinements (one after the other) of samples with different pre-treatments and a parametrically connected refinement of the same measurements. As a simple test only two different states of swelling clay minerals are regarded, air-dried (AD) and ethylene-glycol (EG) intercalated material.

A mixture of two well-known disordered clay minerals was prepared in order to test the applicability of parametric Rietveld refinements for samples containing more than one disordered clay mineral. In addition, 32 samples from a drilling core through a Posidonia shale were analysed.

Rietveld refinements

The *BGMN* software (Bergmann *et al.*, 1998) was used for the Rietveld refinements. The software contains a structure description language, which allows the implementation of physically reasonable disorder models. This interpreter language was used to perform a recursive structure-factor calculation (Ufer *et al.*, 2008), similar to that of the simulation software *DIFFaX* (Treacy *et al.*, 1991). It is also possible, within the interpreter language, to define conditions for the generation of reflection classes. Only reflections with h and $k = 0$ will be included for the refinement of basal reflections, as demonstrated by Ufer *et al.* (2012). Employing this constraint, the *BGMN* program can be used for Rietveld refinements on measurements of oriented mounts.

Refinement procedures with *BGMN* rely on certain input and output text files. The user has to generate a control file (*.sav) that uploads the observed data, a description file for the instrumental contribution of the peak profile and separate structure description files (*.str) for each mineral in the sample. Global parameters such as the degree of the background polynomial and the X-ray wavelength are declared in

the control file. The structure files contain all of the crystallographic data that describe the structure of each mineral such as lattice parameters, atomic position and occupancies, scaling factor, or peak-broadening parameters. In the case of disordered structures, the user can introduce more complex structure descriptions. The refinement results are stored in text files where the user defines the names and paths for the different kinds of data such as diffraction patterns, peak parameters and structural results. The structural results and the peak parameters are generated at the end of the refinement, while the diffraction patterns are updated after each iteration step and can be plotted to track the progress of the refinement visually.

Refineable parameters are declared either as “free” (variable) or fixed, in the control file or the structure description file. It is possible and often recommended to refine a parameter within reasonable limits. The user can also declare additional parameters – global ones in the control file and structural ones, which hold only for the individual structure, in the str-file. All parameters can be connected with each other by analytical functions. The option to declare user-defined parameters and the ability to connect them, allows us to use *BGMN* to perform parametric refinements. Such parameters are included in the co-variance matrix and estimated standard deviations (e.s.d.s) are derived.

Two or more observed diffraction patterns are declared in the control file to perform a parametric refinement. The weighting of the different patterns is performed according to their individual data quality and does not cause any specific problems as long as the statistical quality is of the same magnitude. There are two different ways to assign a set of parameters to an individual measurement. The first is to declare the sets of parameters directly in the structure file. This way is suitable if the patterns contain reflections of the same mineral and only a few parameters vary, e.g. all samples contain quartz, but in different amounts. The same structure file can then be used, with different scaling factors for each measurement.

The second way to define parameters for a parametric refinement is to declare them globally and to hand them over to different structure files for each measurement. This is favoured in the case of strong structural changes in a mineral, which are hard to describe with one structure model, e.g. an air-dried smectite with water molecules in the interlayer and the same smectite in an ethylene glycol-intercalated state. Both structures contain the same parameters regarding the TOT layer, because this is not influenced by the

intercalations. The interlayer structures are completely different and independent of each other. These independent parameters can be defined and refined directly in the structure files without any connections. Other parameters should be declared globally because they are not independent of each other or even the same, as in this example. One of these parameters is, for example, the iron content in the octahedral positions, which is the same for both states and should not vary (Heuser *et al.*, 2013). The models used in this study were described by Ufer *et al.* (2012).

Materials

A mixture of two different swelling clay minerals, a mixed-layer illite-smectite (I-S) and a pure smectite, was prepared. The former, an R1 ordered I-S ISCz-1 from Slovakia is a special clay mineral from the Source Clays Repository of The Clay Minerals Society. It is described as an ordered I-S with an illite:smectite ratio of 70:30. This sample was size fractionated (Atterberg method) to reduce the amount of quartz and other impurities. The material was saturated with Ca cations, after collection of the <2 µm fraction and excess salt was removed by dialysis using deionized water. Traces of quartz and kaolinite were still present in the clay fraction. The chemical formula of ISCz-1 was determined by Ufer *et al.* (2012): ISCz-1: $K_{0.48}Ca_{0.09}(Al_{1.70}Fe_{0.08}Mg_{0.24})[(Si_{3.52}Al_{0.48})O_{10}](OH)_2$.

A bentonite from Peru, S112, was also used to prepare the test mixture. This bentonite consists almost entirely of smectite with only a small quartz impurity (<1 wt.%). ISCz-1 (1.000 g) and Ca-saturated S112 (0.500 g) were mixed and homogenized by wet grinding with ethanol for 2 min in a McCrone mill.

In addition, a series of 32 samples from a drilling core was examined in the same way as the mixture. The material derives from the clayey facies of the Cretaceous Wealden formation in northern Germany. The drilling intersects 300 m with different sub-formations. The sampling of the drilling core was not equidistant and the different numbers for the samples represent the sub-formations. Wealden-5 is only represented by one sample and Wealden-3 and -4 are missing entirely. The samples were size-fractionated and Ca-saturated as described above.

Preparation of oriented mounts

X-ray diffraction (XRD) scans were recorded with 15 mg per cm² clay. An aliquot of 1.5 mL of suspension was deposited on circular (diameter = 2.4 cm) 3 mm

thick ceramic tiles. The suspension was filtered through the tile under vacuum.

XRD analysis of oriented mounts

The XRD pattern were recorded using a PANalytical X'Pert PRO MPD θ - θ diffractometer (Co-K α radiation generated at 40 kV and 40 mA), equipped with a variable divergence slit (20 mm irradiated length), primary and secondary Soller, diffracted beam monochromator and a point detector. The I-S:smectite mixture was measured from 1 to 40°2 θ with a step size of 0.03°2 θ and a measuring time of 6 s/step. All shale samples were investigated from 1–65°2 θ with a step size of 0.03°2 θ and a measuring time of 1 s/step.

The specimens were then stored overnight in an ethylene glycol atmosphere at 60°C. The clay films were measured with the same parameters as the air-dried specimen after cooling to room temperature.

RESULTS AND DISCUSSION

Mixture of illite-smectite and smectite

First, the measurements of the mixture 2/3 illite-smectite ISCz-1 and 1/3 smectite S112 were investigated with independent refinements. A model for Reichweite 1 (R1) ordering of the I-S was chosen according to Ufer *et al.* (2012). This model describes mixed layering of illitic layers with potassium in the interlayer and smectitic layers with calcium and water in the interlayer. Two different hydration states can be considered: a mono-layer and a bi-layer of water. Refineable structural parameters are layer thicknesses, proportion of illitic layers (*wI*), proportion of smectitic mono-layer and bi-layers of water, probability *pII* that an illitic layer follows another illitic layer and the occupancies of iron in the octahedral site and K, Ca and H₂O in the interlayer space. The interstratifications are typically dominated by illitic layers; ordering of hydration stages of smectitic interlayers was not taken into consideration and a double layer ethylene glycol complex was assumed for simplicity. The pure smectite was also described with two interlayer hydration states, refineable proportion and layer thickness of these two states and refineable occupancies of iron in the octahedral site and Ca and H₂O in the interlayer space. Scaling and separate 001 and *hkl* peak-broadening parameters were refined as non-structural parameters.

The patterns observed showed weak, non-basal peaks for the two layer silicates, which were described in sum with a strongly restrained model for turbostratically disordered dioctahedral smectites. Only the scale factor, the constrained *a*–*b* lattice parameters and the isotropic line broadening were refined. Quartz and kaolinite impurity peaks and some corundum peaks from the ceramic tile were described with standard Rietveld models. The measurement of the ethylene glycol-intercalated material was refined with the corresponding models, by replacing the water layers with an interlayer structure model of a double layer of EG molecules. Evidently some of the parameters of the two refinements should lead to the same results, as they describe the same mineral. These relevant parameters are listed in Table 1, and the refinement patterns are shown in Fig. 1 (upper). The observed and the calculated diffraction lines are in good agreement for both refinements and the numerical results although quite close, are significantly different, considering the e.s.d.s. Obviously, at least one of them is incorrect.

A parametric refinement of the same measurements was performed after the independent refinements. Parameters of the I-S and smectite models of the two states, which should be the same, were declared as global parameters and were handed over to the corresponding structure models. These parameters were the stacking parameters *wI* and *pII*, the illitic layer thickness *lI* and the occupancies *pFe*, *pK* and *pCa* of the I-S and *pFe* and *pCa* of the smectite. All other refined structural parameters of the two states were independent of each other and were thus refined directly in the structure file. The structural parameters of the models for quartz, kaolinite and corundum did not change due to the sample pre-treatment and consequently should not be refined independently. The changes are not significant for the low-intensity non-basal reflections of the smectite and the structure model was not refined. Parameters could be declared directly in the structure file and were valid for both measurements. Even the scaling factor could be regarded as the same for both states, because the measurement conditions did not change. For this reason the peak intensities of pre-treatment minerals are practically identical.

Two refinement patterns of the parametric refinement are shown in Fig. 1 (lower). The agreement of observed and calculated data is again satisfying and it is difficult to observe a difference in the quality of the independent and the parametric refinements. As expected, the parametric refinement led to a slightly

TABLE 1. Comparison of the results of the independent and parametric refinements.

	AD, independent	EG, independent	AD, parametric	EG, parametric
no param.	42	43		63
steps	28	53		18
time	1 min 43 s	3 min 17 s		3 min 3 s
R_{wp}	6.11%	6.37%	6.88%	7.30%
wI	64.45(17)%	66.15(17)%		65.84(14)%
pII	0.5284(23)	0.4882(34)		0.5294(22)
tI	10.0003(32) Å	9.9828(29) Å		10.0072(27) Å
pFe	0.1086(60)	0.1222(54)		0.1313(49)
pCa	0.3*	0.3*		0.3*
pK	0.65*	0.65*		0.65*
pFe (Smectite)	0*	0.031(20)		0.011(17)
pCa (Smectite)	0.3*	0.3*		0.3*

* parameter reached the limit of the restraint.

AD: air-dried state, EG: ethylene glycol-saturated.

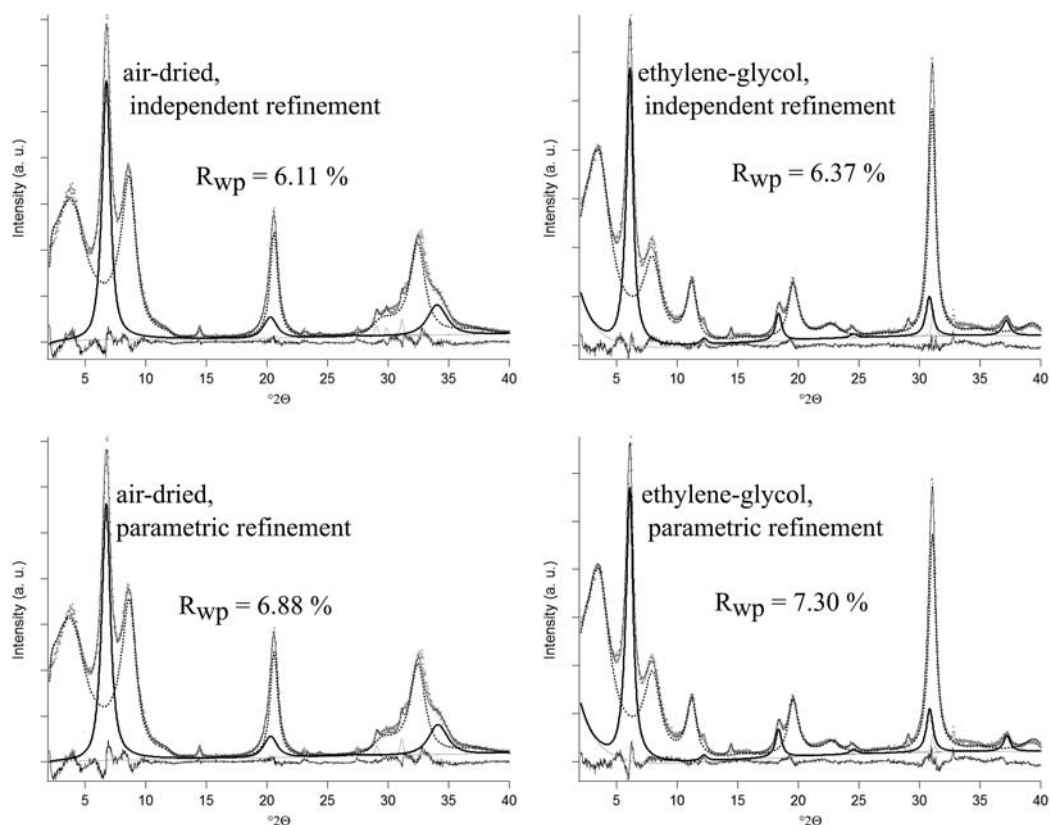


FIG. 1. Refinement patterns of the mixture ISCz-1 and smectite. Upper: independent refinements. Lower: parametric refinements. Left: AD material. Right: EG intercalated material. Thick black line: smectite. Dotted black line: I-S. All impurity peaks are drawn as thin grey lines.

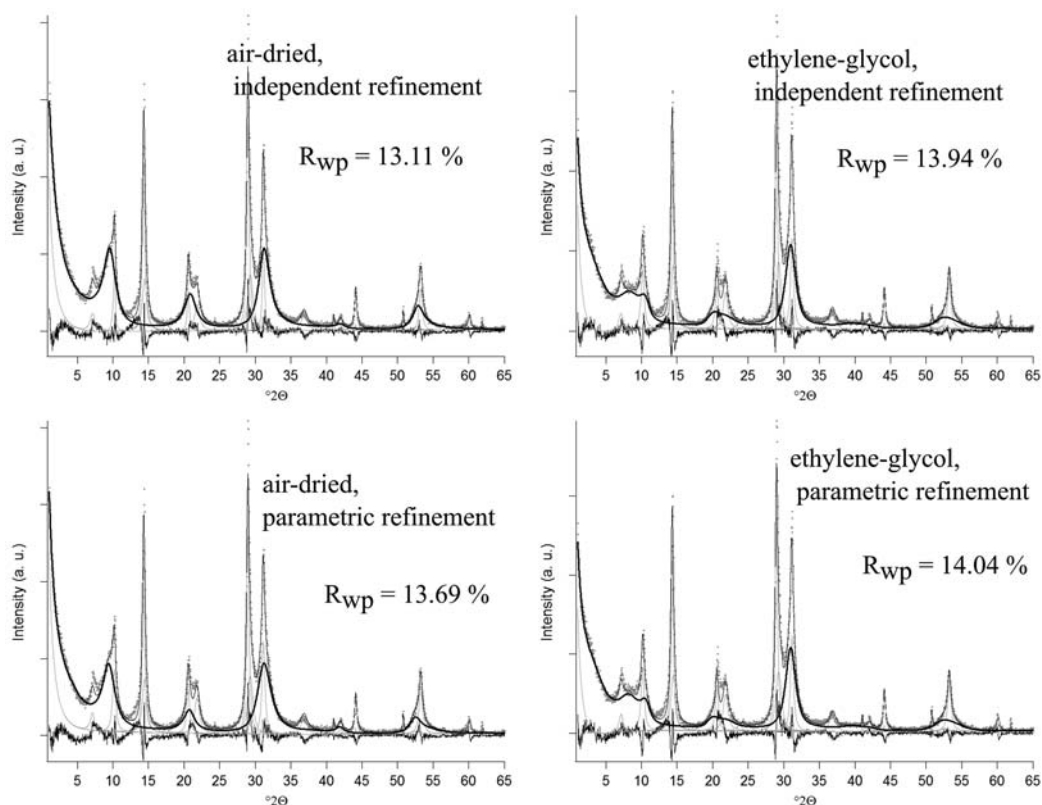


FIG. 2. Refinement patterns of a shale sample (132.10 m). Upper: independent refinements. Lower: parametric refinements. Left: AD material. Right: EG intercalated material. Thick black line: illite-smectite. All other patterns are drawn as thin grey lines.

worse agreement parameter R_{wp} between the observed and calculated patterns.

The number of refineable parameters of the parametric refinement is smaller than the sum of parameters of the two independent refinements, even though the same parameters were refined. The number decreases because some parameters were shared between the two states. Calculation time per iteration step is greater for the parametric refinement due to the greater calculation effort, but the total calculation time clearly decreases compared with the sum of the two independent refinements.

Parametric refinement led to structural results which are valid for both states. Notably the values are not simply a mean value of the independent results. In some cases they actually lay outside the range of the independent results.

Occupancy parameters tend to reach one of the refinement limits for the independent refinements as well as for the parametric refinement.

Shale samples

The 32 shale samples contain mixed-layer I-S, muscovite, kaolinite, chlorite and quartz; while two samples also contained calcite. Corundum peaks were again visible due to reflections from the ceramic tile. All patterns are quite similar and significant differences in the shape of the I-S patterns were barely visible. Preliminary tests showed that the application of an R1-ordered model for I-S led to satisfying results. Models for R2- and R3-ordering were not suitable.

The models for the two states of the I-S were identical to those for the refinement of the mixture. The starting values and limitations of all refineable parameters were identical for all samples. The muscovite, chlorite and kaolinite were described as having ordered stacking. Standard structure models were used for quartz, calcite and corundum.

Independent refinements were compared with a parametric refinement again. Figure 2, for example,

TABLE 2. Comparison of structural results of the independent and parametric refinements for a sample series from the clayey facies of the Cretaceous Wealden formation in northern Germany. Left: iron occupancy pFE. Middle and Right: stacking parameters wI and pII.

Sub-formation	Depth [m]	pFE (param.)	pFE (AD ind.)	pFE (EG ind.)	wI (param.)	wI (AD ind.)	wI (EG ind.)	pII (param.)	pII(AD ind.)	pII (EG ind.)
Wealden-6	73.80	0.14(1)	0.09(1)	0.12(2)	0.788(6)	0.805(6)	0.817(7)	0.732(8)	0.780(8)	0.776(10)
	81.32	0.14(1)	0.10(1)	0.17(2)	0.817(5)	0.826(5)	0.830(1)	0.776(7)	0.812(6)	0.795(2)
	92.25	0.23(2)	0.20(2)	0.22(2)	0.769(7)	0.774(8)	0.7924(8)	0.72(1)	0.74(1)	0.74(1)
	100.00	0.14(2)	0.17(2)	0.18(2)	0.757(7)	0.753(7)	0.787(10)	0.69(1)	0.71(1)	0.73(2)
	110.82	0.22(2)	0.20(2)	0.23(2)	0.757(6)	0.773(7)	0.781(11)	0.704(8)	0.742(9)	0.721(16)
	117.95	0.20(1)	0.14(1)	0.22(2)	0.801(4)	0.810(5)	0.827(1)	0.752(6)	0.784(8)	0.790(2)
	126.00	0.18(1)	0.13(1)	0.17(2)	0.801(6)	0.803(5)	0.822(7)	0.752(9)	0.777(8)	0.783(10)
	132.10	0.15(1)	0.11(1)	0.14(2)	0.807(4)	0.806(5)	0.823(1)	0.763(7)	0.785(7)	0.785(2)
138.95	0.21(1)	0.14(1)	0.21(2)	0.793(4)	0.799(6)	0.816(7)	0.742(7)	0.781(8)	0.774(10)	
Wealden-5	146.80	0.14(3)	0.18(6)	0.15(3)	0.709(7)	0.762(5)	0.757(11)	0.638(10)	0.728(7)	0.678(19)
Wealden-2	314.50	0.16(1)	0.082(9)	0.19(2)	0.814(4)	0.823(5)	0.830(1)	0.772(6)	0.813(7)	0.796(2)
	318.80	0.142(9)	0.08(1)	0.15(2)	0.804(4)	0.816(5)	0.826(1)	0.759(6)	0.804(7)	0.789(2)
	323.60	0.22(2)	0.22(2)	0.30(3)	0.789(6)	0.787(8)	0.814(9)	0.757(9)	0.779(9)	0.771(13)
	326.70	0.151(9)	0.08(1)	0.17(1)	0.806(4)	0.812(5)	0.831(1)	0.764(6)	0.802(2)	0.797(2)
	332.70	0.171(9)	0.088(9)	0.17(2)	0.811(4)	0.808(6)	0.821(2)	0.770(6)	0.798(8)	0.783(2)
	337.60	0.23(2)	0.20(2)	0.08(3)	0.750(6)	0.772(8)	0.793(12)	0.711(8)	0.756(9)	0.739(18)
	341.70	0.117(9)	0.07(1)	0.15(2)	0.806(4)	0.818(5)	0.819(7)	0.759(6)	0.797(6)	0.780(10)
	347.30	0.22(1)	0.10(1)	0.23(2)	0.811(3)	0.808(6)	0.827(6)	0.767(7)	0.787(7)	0.791(9)
Wealden-1	349.50	0.28(2)	0.21(2)	0.27(3)	0.795(6)	0.796(7)	0.826(2)	0.760(8)	0.776(10)	0.790(3)
	353.64	0.27(3)	0.22(3)	0.3*	0.760(8)	0.777(9)	0.658(17)	0.73(1)	0.76(1)	0.50(3)
	357.70	0.23(1)	0.20(2)	0.28(2)	0.818(4)	0.810(6)	0.830(1)	0.778(5)	0.795(7)	0.795(2)
	363.60	0.34(3)	0.34(3)	0.30(6)	0.765(8)	0.779(12)	0.791(16)	0.74(1)	0.76(1)	0.74(2)
	366.50	0.27(3)	0.26(2)	0.13(6)	0.765(7)	0.783(10)	0.713(21)	0.737(9)	0.762(12)	0.62(3)
	368.60	0.21(2)	0.27(2)	0.14(3)	0.770(6)	0.785(8)	0.808(3)	0.730(8)	0.763(9)	0.762(5)
	370.50	0.28(2)	0.19(2)	0.19(5)	0.773(7)	0.777(8)	0.795(17)	0.747(8)	0.760(9)	0.742(23)

(continued)

TABLE 2. (contd.)

Sub-formation	Depth [m]	pFE (param.)	pFE (AD ind.)	pFE (EG ind.)	wI (param.)	wI (AD ind.)	wI (EG ind.)	pII (param.)	pII (AD ind.)	pII (EG ind.)
	372.40	0.20(2)	0.29(4)	0.21(5)	0.780(9)	0.798(12)	0.804(16)	0.75(1)	0.78(1)	0.76(2)
	374.75	0.23(2)	0.29(2)	0.22(4)	0.790(6)	0.786(8)	0.816(13)	0.759(8)	0.767(9)	0.780(17)
	374.60	0.43(3)	0.42(3)	0.3*	0.78(1)	0.79(1)	0.790(13)	0.76(2)	0.78(2)	0.75(2)
	375.29	0.20(2)	0.18(2)	0.05(3)	0.754(6)	0.806(9)	0.794(13)	0.724(8)	0.790(10)	0.741(20)
	378.50	0.20(2)	0.30(4)	0.3*	0.780(6)	0.802(7)	0.787(11)	0.735(8)	0.778(8)	0.729(18)
	379.60	0.32(2)	0.40(3)	0.3*	0.783(8)	0.766(11)	0.820(2)	0.75(1)	0.75(1)	0.781(4)
	382.50	0.13(1)	0.16(1)	0.08(1)	0.788(4)	0.792(4)	0.8203(2)	0.735(5)	0.754(6)	0.781(2)

* parameter reached the limit of the restraint.

shows a comparison of all refined patterns for one sample. All fits are visually of comparable quality and only a slightly smaller R_{wp} value indicates that the independent refinements led to a slightly better fit. Table 2 shows some refinement results.

Convergence behaviour

The mean calculation time per step of the parametric refinement was 1.70 s, which is nearly the sum of the two independent values (1.00 s/step + 0.76 s/step). However, the total calculation time of the parametric refinements is lower because the mean number of iteration steps is less than the sum of the two independent ones.

Some refinements needed extremely long calculation times, due to a large number of iteration steps (>100). Even the parametric refinement showed cases with an extremely large number of steps. For example, one parametric refinement took 21 min with 712 steps, while the corresponding two independent refinements were performed within only 52 s (AD state) plus 5 min 34 s (497 steps). There are other cases in which one of the independent refinements was extremely long while the parametric refinement of the same measurements was faster than the average. Therefore, the notion that time might be saved by independent refinements is not universally valid. However, it may be valid, on average, for a series of many samples.

Relevance of results

Table 2 shows a comparison of results of the refinement of structural parameters. Much larger differences of the iron occupancy were found than in the previous example. The pFE of sample 337.60 m is 0.20(2), according to the independent refinement of the AD state, while it is only 0.08(3) in the case of the EG state. The result from parametric refinement lies outside this range at 0.23(2). Again the result from parametric refinement is not simply a mean value and it is identical to that of the independent one of the AD state, considering the e.s.d.

Differences in the stacking parameters wI and pII are difficult to interpret and the values were therefore plotted in a junction probability diagram for R1 (Fig. 3, Bethke *et al.*, 1986). The probability that an illitic layer follows another illitic layer, pII, is plotted against the proportion of illitic layers in a stack, wI. For wI = pII, a point plots on the line for R1 random ordering, equivalent to R0 disorder. Points below this line show a tendency to order. The maximum possible degree of ordering (mpdo) is reached at the line for R1, ordered.

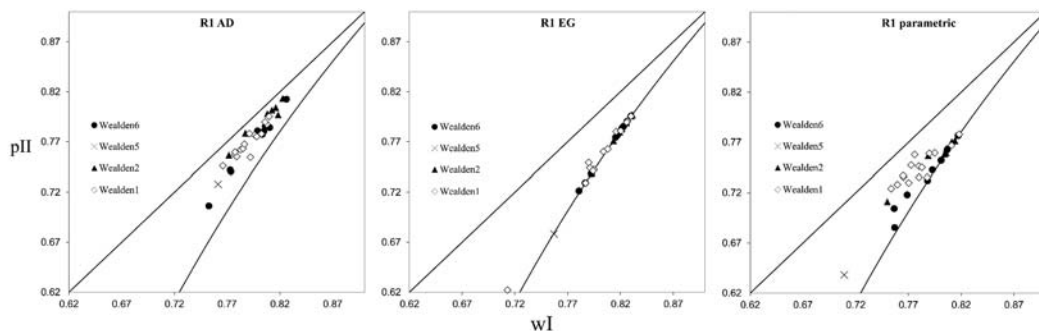


Fig. 3. Junction probability diagrams of the refinement results for pII and wI. Left: independent refinement, AD state. Middle: independent refinement, EG state. Right: parametric refinement.

Stacks that plot on this line do not contain the smectite-smectite sequence. Points below this line are physically impossible. Refinement limits of pII were defined with a dependance on wI to avoid these physically forbidden results.

Figure 3 (left) shows that all refined values of the independent refinement of the AD state plot between the two lines. This means that the stacking shows a certain degree of ordering, but not the maximum possible one. In contrast to that, the results of the independent refinement of the EG state all plot on, or quite near to, the R1, ordered line (Fig. 3, middle). Accordingly, the two independent refinements did not lead to a consistent result regarding the degree of ordering.

The parametric refinement results of these parameters (Fig. 3, right) plot partially on or near the R1, ordered line. Other points plot in between the random and ordered stacking points. Considering the stratigraphic origin of the samples, it seems that the samples from the Wealden-1 sub-formation plot mainly in between the lines, while the other sub-formations tend to lie closer to, or on the line of maximum ordering. Such differentiation may be interesting, even if there is no clear geological explanation at the moment.

CONCLUSIONS

Rietveld refinements have the advantage that they lead to a user-independent result without tedious manual optimization of parameters. Nevertheless, the independent refinements of samples measured under different conditions may also lead to inconsistent results. In contrast to this, parametric refinement necessarily produces results that are consistent for several states. A comparison of the fits of the

diffraction patterns showed agreements that are difficult to evaluate visually. Only examination of the statistical quality parameters showed that the fits of the parametric refinements are slightly worse on constraining with more than one dataset, but the user gains an overall result free from contradictions. In rare cases the parametric refinement may obtain a fit with a smaller R_{wp} value, because the independent refinement ended in a local minimum.

Parametric refinement was often faster than the sum for the independent results, even though the calculation time per iteration was longer due to a greater calculation effort. The reason for this is that the parametric refinement typically needed fewer iteration steps for convergence. This observation, however, is not universally true, as some examples in this study have shown. However, in general, it might be valid for larger sets of samples.

The results from parametric refinements were not necessarily an average value of the results of the independent refinements and it could be demonstrated that in several cases it can even run outside the range of the results from the independent refinements.

The refinement of the intensity-affecting parameters like occupancies often reached the refinement limits, as already described by Ufer *et al.* (2012). Furthermore, this could not be prevented by parametric refinement and was probably a result of correlations. More complex models containing further constraints between different sample states may help to achieve unique results for all parameters. For example the use of a general model describing the interlayer water content as a function of the relative humidity, combined with measurements at controlled humidity, could help to reduce correlation between occupancies of interlayer cations and water molecules.

Parameters affecting the peak positions such as wI and pII can be refined with greater reliability than the intensity-affecting parameters. However, it was not possible for the values for the shale samples in this study to refine consistently for the ordering of the stacking sequence from the air-dried and ethylene glycol-saturated sample states. In contrast, the parametric refinements led to results that can distinguish slight differences of ordering. The group of samples with a lesser degree of ordering could be attributed to another stratigraphical level than samples showing a maximum possible degree of ordering. The significance of this observation will be verified by further geochemical examinations.

The examples shown here were quite simple and they only used the fact that some structural parameters change systematically while others do not. Other possible applications are to determine mineral contents in different size fractions, or for additional intercalations, or for identifying structural changes on heating.

REFERENCES

- Bergmann J., Friedel P. & Kleeberg R. (1998) BGMN - a new fundamental parameter based Rietveld program for laboratory X-ray sources, its use in quantitative analysis and structure investigations. *CPD Newsletter, Commission of Powder Diffraction, International Union of Crystallography*, **20**, 5–8.
- Bethke C.M., Vergo N. & Altaner S.P. (1986) Pathways of smectite illitization. *Clays and Clay Minerals*, **34**, 125–135.
- Drits, V.A. & Tchoubar, C. (1990) *X-ray Diffraction by Disordered Lamellar Structures*. Springer, Berlin Heidelberg, 371p.
- Heuser M., Andrieux P., Petit S. & Stanjek H. (2013) Iron-bearing smectites: a revised relationship between structural Fe, b cell edge lengths and refractive indices. *Clay Minerals*, **48**, 97–103.
- Rajiv P., Dinnebier R.E., Jansen M. & Joswig M. (2011) Automated parametric Rietveld refinement: Applications in reaction kinetics and in the extraction of microstructural information. *Powder Diffraction Supplement*, **26**, (S1), S26–37.
- Reynolds R.C. Jr. (1983) Calculation of absolute diffraction intensities for mixed-layered clays. *Clays and Clay Minerals*, **31**, 233–234.
- Reynolds R.C. Jr. (1985) NEWMOD[®] a computer program for the calculation of one-dimensional diffraction patterns of mixed-layered clays. R.C. Reynolds, Jr., 8 Brook Rd., Hanover, NH, USA.
- Sakharov B.A., Lindgreen H., Salyn A., and Drits V.A. (1999) Determination of illite-smectite structures using multispecimen X-ray diffraction profile fitting. *Clays and Clay Minerals*, **47**, 555–566.
- Stinton G.W. & Evans J.S.O. (2007) Parametric Rietveld refinement. *Journal of Applied Crystallography*, **40**, 87–95.
- Treacy M.M.J., Newsam J.M. & Deem M.W. (1991) A general recursion method for calculating diffracted intensities from crystals containing planar faults. *Proceedings of the Royal Society, London*, **A433**, 499–520.
- Ufer K., Kleeberg R., Bergmann J., Curtius H. & Dohrmann R. (2008) Refining real structure parameters of disordered layer structures within the Rietveld method. *Zeitschrift für Kristallographie*, **27**, 151–158.
- Ufer K., Kleeberg R., Bergmann J. & Dohrmann R. (2012) Rietveld refinement of disordered illite-smectite mixed-layer structures by a recursive algorithm – I: One-dimensional patterns. *Clays and Clay Minerals*, **60**, 507–534.